

# Microscale Flow Dynamics of Red Blood Cells in Microchannels: An Experimental and Numerical Analysis

R. Lima, C.S. Fernandes, R. Dias, T. Ishikawa, Y. Imai, and T. Yamaguchi

**Abstract** The blood flow dynamics in microcirculation depends strongly on the microvascular networks composed with short irregular vessel segments which are linked by numerous bifurcations. This paper presents the application of a confocal micro-PTV system to track RBCs through a rectangular polydimethylsiloxane (PDMS) microchannel with a bifurcation. By using a confocal micro-PTV system, we have measured the effect of bifurcation on the flow behaviour of both fluorescent particles diluted in pure water and RBCs in concentrated suspensions. After performing simulations with the commercial finite element software package POLYFLOW<sup>®</sup>, some experimental results were compared with the numerical results and the limitations of these simulations were outlined.

**Keywords** Blood flow · Microvascular networks · Bifurcation · Microchannel

---

R. Lima (✉) and R. Dias  
ESTiG, IPB, C. Sta. Apolonia, 5301-857 Braganca, Portugal  
e-mail: [ruimec@ipb.pt](mailto:ruimec@ipb.pt); [ricardod@ipb.pt](mailto:ricardod@ipb.pt)

and  
CEFT, FEUP, R. Dr. Roberto Frias, 4200-465 Porto, Portugal

C.S. Fernandes  
ESTiG, IPB, C. Sta. Apolonia, 5301-857 Braganca, Portugal  
e-mail: [cveiga@ipb.pt](mailto:cveiga@ipb.pt)

T. Ishikawa and Y. Imai  
Department of Bioengineering & Robotics, Graduate School of Engineering,  
Tohoku University, 6-6-01 Aoba, 980-8579 Sendai, Japan  
e-mail: [ishikawa@pfs1.mech.tohoku.ac.jp](mailto:ishikawa@pfs1.mech.tohoku.ac.jp); [yimai@pfs1.mech.tohoku.ac.jp](mailto:yimai@pfs1.mech.tohoku.ac.jp)

T. Yamaguchi  
Department of Biomedical Engineering, Graduate School of Engineering,  
Tohoku University, 6-6-01 Aoba, 980-8579 Sendai, Japan  
e-mail: [takami@pfs1.mech.tohoku.ac.jp](mailto:takami@pfs1.mech.tohoku.ac.jp)

# 1 Introduction

The phenomena of blood flow in microvessels (diameters less than  $300\ \mu\text{m}$ ) are crucial in maintaining healthy organs and tissues. Although these phenomena have been studied for many years it still remains incompletely understood [25]. It is therefore important to investigate the behaviour of blood flow occurring at microvessels in order to better understand the role of blood cells in the process of delivering oxygen and materials to the organs and tissues.

The complexity to control and obtain reliable measurements of the blood flow behaviour through the *in vivo* microvascular system has led several researchers to perform their studies by using narrow glass tubes with simple geometries. By using *in vitro* models it allows a more precise control over the experimental variables of interest and extracts detailed information of the flow behaviour of individual blood cells. In fact, much of the understanding of the haemodynamics phenomena observed in microcirculation was obtained from studies on the both macro and microrheology properties of blood flowing through glass microtubes [3, 11, 13, 16, 17, 25].

Although glass microchannels present certain similarities to *in vivo* microcirculation, it is also clear that these kind of *in vitro* experiments differ from microvessels in several respects, such as: elasticity of microvessels, effect of the endothelial surface layer and microvascular networks composed with short irregular vessel segments which are linked by numerous bifurcations. Thus it was not surprising that several studies on blood flow in glass microtubes and in microvessels have yielded conflicting results with respect to blood viscosity [20] and flow resistance [27]. Hence, the rheological properties of blood should not be only interpreted from measurements in viscometers and microtubes with simple geometries.

*In vivo* microvascular networks are composed of many divergent microvascular bifurcations which likely influence the blood flow behaviour in the microcirculation. In the present work, a confocal micro-PTV system is used to measure the blood flow through a symmetric PDMS bifurcation fabricated by soft lithography. Moreover, the experimental data were compared numerically by using the commercial finite element software package POLYFLOW<sup>®</sup>. By using this combination we expect to gain understanding about several important parameters that affect the blood flow through a diverging microvessel bifurcation.

## 2 Materials and Methods

### 2.1 Fabrication of the Microchannels

The microchannels will be manufactured in polydimethylsiloxane (PDMS) due to their advantageous properties, including good optical transparency and biocompatibility, easily reversible sealing to glass, elasticity, replication of fine and complex

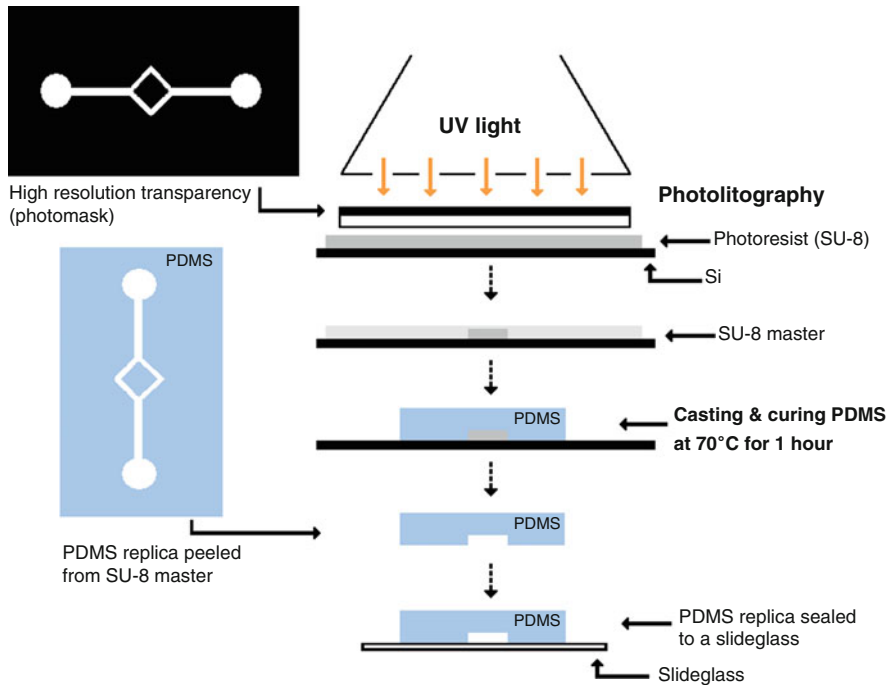


**Fig. 1** Main steps of the soft lithographic technique to manufacture a microchannel with a symmetrical bifurcation geometry

geometries, and high gas permeability which is suitable for culturing cells inside the microchannels [17]. The procedure to manufacture the PDMS microchannel with a symmetric bifurcation is illustrated in Fig. 1. Briefly, the microchannel geometry was designed using a CAD system, and a high resolution (25,400 dpi) photomask was printed on plastic (polyester) transparencies at CAD/Art Services, Inc. (Bandon, USA). By applying a photolithographic technique (see Fig. 1), a solid master was fabricated on a silicon (Si) wafer with an ultrathick photoresist (SU-8). In this process, by using a spin-coating technique, a thin layer of SU-8 photoresist was coated on Si wafer and then patterned by UV exposure through the photomask. Using a SU-8 developer, it was possible to obtain the desired mold master. Then, metal wire posts were placed on the SU-8 mold master to create the connection channels to the input/output ports. The PDMS was made by mixing a base and curing agent (Silpot 184; Dow Corning, USA) at a weight ratio of 10:1. After removing the bubbles created during mixing, the PDMS was poured over the mold master and baked on a hot plate for about 1 h at 70 °C. Both master and PDMS were then cooled to room temperature and the PDMS design and embedded metal wire posts were removed from the SU-8 master and PDMS, respectively. Finally, the three-dimensional PDMS microchannel structure was cleaned with ethanol and brought into contact with a clean slide glass, where a reversible seal

was formed spontaneously. The input/output ports were made by means of a 200  $\mu\text{l}$  micro-pipette tip. This tip was inserted tightly into the connection channels where it exerts pressure on the PDMS and provides a liquid proof seal. Top tubes were also fitted tightly into the micro-pipette tip in order to deliver the working fluids from the syringe pump. Due to the elasticity of the connection tubes and conical shape of the tip, we did not observe any fluid leakage during our experiments [17].

## 2.2 Working Fluids and Geometry of the Bifurcation

Two working fluids were used in this study: pure water and dextran 40 (Dx40) containing about 14% (14Hct) of human red blood cells (RBCs). The blood was collected from a healthy adult volunteer, where ethylenediaminetetraacetic acid (EDTA) was added to prevent coagulation. The RBCs were separated from the bulk blood by centrifugation and aspiration and then washed twice with physiological saline (PS). The washed RBCs were labeled with a fluorescent cell tracker (CM-Dil, C-7000, Molecular Probes) and then diluted with Dx40 to make up the required RBCs concentration by volume. All blood samples were stored hermetical at 4  $^{\circ}\text{C}$  until the experiment was performed at controlled temperature of about 37  $^{\circ}\text{C}$  [13].

The geometry and dimensions of the microchannel bifurcation is illustrated in Fig. 2. In the present study we decided to use the following dimensions: 150  $\mu\text{m}$  wide for parent vessel ( $W_0$ ); 75  $\mu\text{m}$  wide for daughter vessel ( $W_1 = W_2 = 1/2W_0$ ) and 50  $\mu\text{m}$  deep.

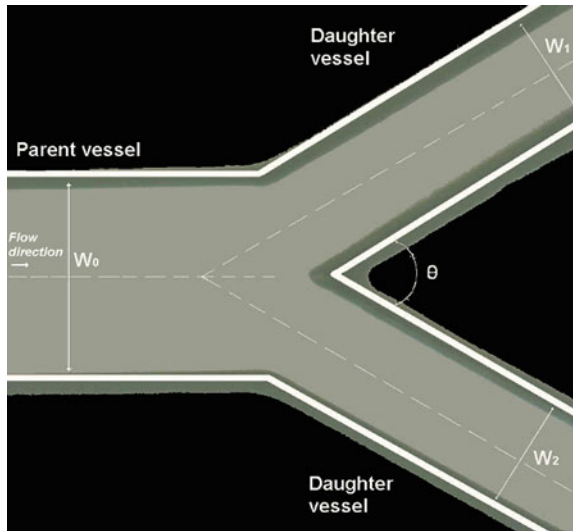


**Fig. 2** Symmetrical bifurcation geometry used in this study:  $W_0 = 150 \mu\text{m}$ ,  $W_1 = W_2 = 75 \mu\text{m}$ ,  $\theta = 60^{\circ}$ , depth = 50  $\mu\text{m}$

**Table 1** Experimental parameters used to calculate the Re

Density (kg/m <sup>3</sup> )	1,046
Mean velocity (m/s)	$3.8 \times 10^{-4}$
Hydraulic diameter (m)	$7.5 \times 10^{-5}$
Viscosity of Dx-40 (Ns/m <sup>2</sup> )	$4.5 \times 10^{-3}$
Re	0.007

### 2.3 Confocal Micro-PTV Experimental Set-Up

The confocal micro-PTV system used in our experiment consists of an inverted microscope (IX71, Olympus, Japan) combined with a confocal scanning unit (CSU22, Yokogawa) and a diode-pumped solid state (DPSS) laser (Laser Quantum Ltd) with an excitation wavelength of 532 nm. Moreover, a high-speed camera (Phantom v7.1) was connected into the outlet port of the CSU22. The microchannel was placed on the stage of the inverted microscope where the flow rate of the working fluids was kept constant ( $Re = 0.007$ ) by means of a syringe pump (KD Scientific Inc.). The Reynolds number ( $Re$ ) and associated experimental parameters are summarized in Table 1. A thermo plate controller (Tokai Hit) was set to 37 °C. All the confocal images were captured in the middle of the microchannels with a resolution of  $640 \times 480$  pixels, at a rate of 100 frames/s with an exposure time of 9.4 ms. The recorded images were transferred to the computer and then evaluated in the Image J (NIH) [1] by using the manual tracking MtrackJ [21] plugin. As a result it was possible to track single RBCs through the middle plane of the microchannel (Fig. 3).

### 2.4 Simulation Method

The numerical calculations for the laminar isothermal flow of pure water were performed using the finite-element computational fluid dynamics (CFD) program POLYFLOW<sup>®</sup>. The simulations were carried out in a 3D geometry representing the microchannel (see Fig. 4). The mesh used in the simulations was mainly constituted by quadrilateral elements, the discretization of the walls of the channel being presented in Fig. 4. The size of the elements was fixed after a grid independence test. The grids were successively refined and the velocity obtained with the different meshes were compared, the results being considered independent of the mesh when a difference below 1% was achieved [4, 8–10].

The equations solved were the conservation of mass and momentum equations for laminar incompressible flow of water. The problem is a non-linear problem, so it was necessary to use an iterative method to solve the referred equations. In order to evaluate the convergence of this process; a test based on the relative error in the velocity field was performed. For the velocity field, the modification on each node between two consecutive iterations is compared to the value of the velocity at the current iteration. In the present work, the convergence value was set to  $10^{-4}$ , since this value is appropriate for the studied problem [5, 8–10].

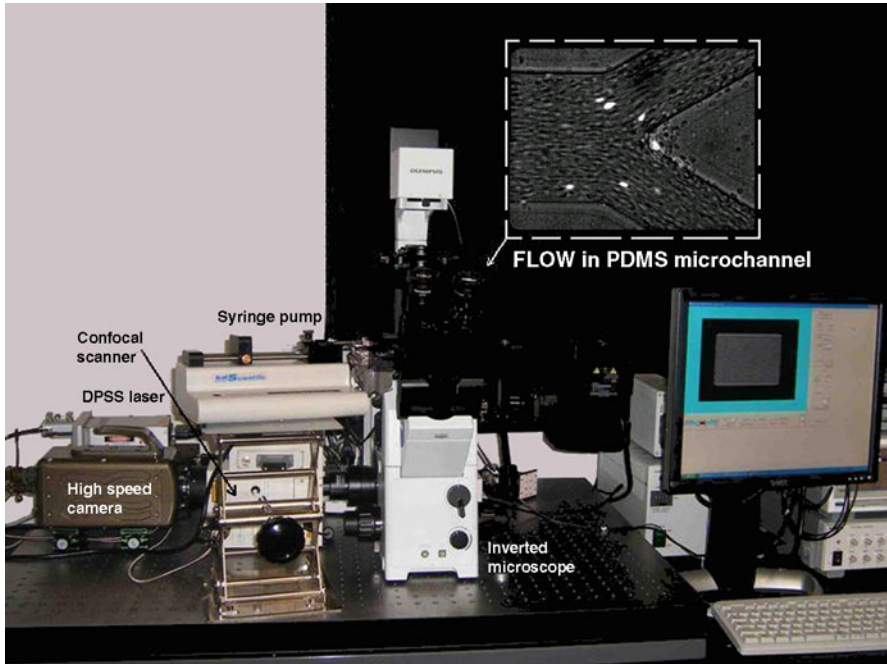


Fig. 3 Experimental set-up

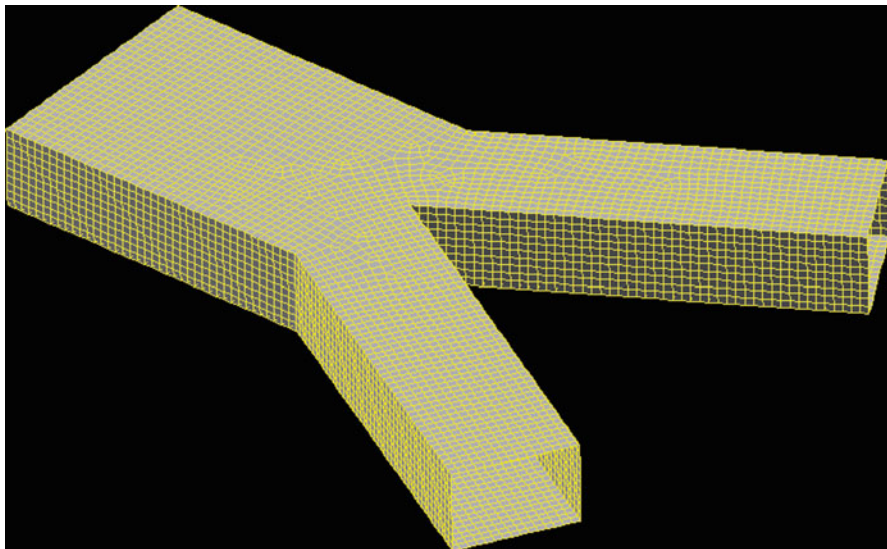


Fig. 4 Computational domain and mesh used

**Table 2** Rheological parameters of blood [12]

Rheological model	$\eta$ (Pa.s)	$K$ (-)	$n$ (-)	$\lambda$ (s)	$\eta_\infty$ (Pa.s)	$\eta_0$ (Pa.s)
Newtonian	0.00345	-	-	-	-	-
Power law model	-	0.035	0.6	-	-	-
Carreau model	-	-	0.3568	3.313	0.00345	0.056

The boundary conditions were established in order to reproduce the experimental conditions. The geometry of the bifurcation was idealized and close to the original dimensions of the photomask. Additionally, the mean velocity at the inlet of the microchannel was  $3.8 \times 10^{-4}$  m/s and slip at the walls of the channel was assumed to be non-existent. The referred velocity was imposed considering a constant flow rate on the referred boundary.

In the numerical study, blood was considered a Newtonian and non-Newtonian fluid. In the last case, the rheology of the blood was described by two different constitutive models – power law model and the Carreau model [12] – which are, respectively, traduced mathematically by the equations:

$$\eta = K \dot{\gamma}^{n-1}, \quad (1)$$

$$\eta = \eta_\infty + (\eta_0 - \eta_\infty) \left[ 1 + (\lambda \dot{\gamma})^2 \right]^{(n-1)/2}, \quad (2)$$

where  $\eta$  is the viscosity of the fluid,  $K$  the consistency index,  $n$  the flow index behavior,  $\dot{\gamma}$  the shear rate,  $\eta_\infty$  the viscosity for high shear rates,  $\eta_0$  the viscosity for low shear rates and  $\lambda$  the natural time. For the blood, the rheological parameters present in the above equations are reported in Table 2.

### 3 Results and Discussion

The confocal micro-PIV system was first evaluated by comparing the experimental results not only with a well established analytical solution for steady flow in a rectangular microchannel [15] but also with a reliable numerical method that was used in past investigations to study the flow behaviour of Newtonian or non-Newtonian fluids at low Reynolds numbers [9, 10].

The numerical, experimental and analytical results of the present work were obtained for the middle plane (25  $\mu$ m height) of the rectangular microchannel. The averaged velocity data obtained from the confocal micro-PTV measurements, analytical solution and numerical simulation were in good agreement. A more detail description of these results can be found elsewhere [22].

By using a confocal micro-PTV system it was possible to obtain series of successive images at the middle of the bifurcation. Figures 5a and 6 show images with both fluorescent particles and labeled RBCs (laser-emitted light) flowing through a symmetric bifurcation, together with the correspondent time position tracking of both



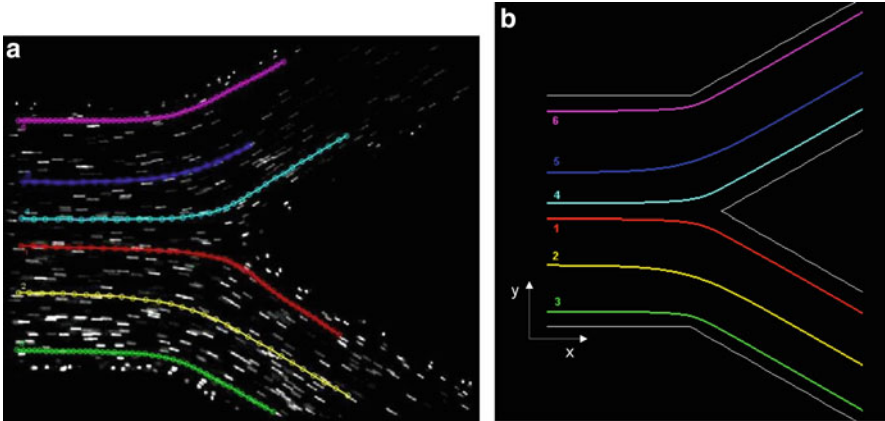


**Fig. 5** (a) Paths displacement of fluorescent particles flowing in pure water; (b) Numerical trajectories using pure water

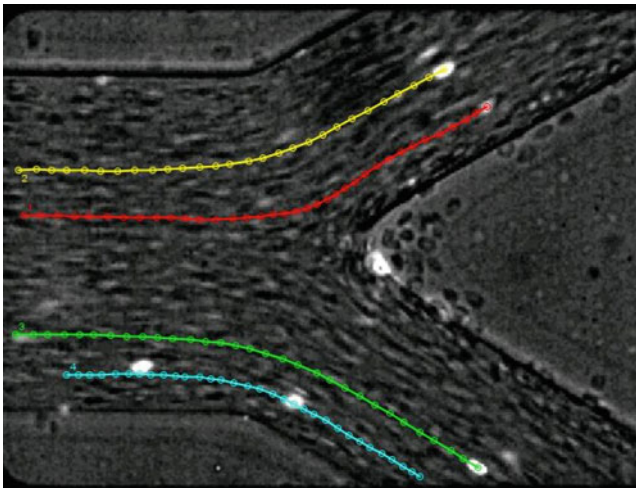


**Fig. 6** Paths displacement of labeled RBCs (*bright spots*) flowing in physiological fluid with 14% Hct (32 $\times$ )

particles and individual RBCs. Qualitative comparison between the experimental data from pure water (see Fig. 5a) and the numerical simulation (see Fig. 5b), shows that in both cases the trajectories do not exhibit any appreciable deviations in the transversal ( $yy$  axis) direction.

In addition by comparing qualitatively the experimental data from both pure water and in vitro blood (14% Hct) it is possible to observe that some RBC paths seems



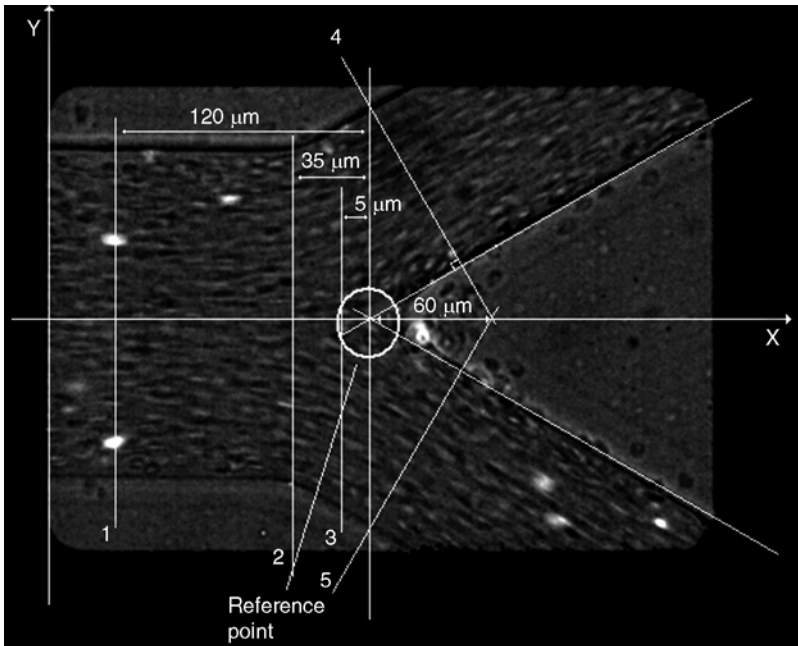


**Fig. 7** Regions where the velocity profiles of the numerical and experimental results were compared

to suffer small deviations from the streamlines of the plasma flow probably due to flow perturbations caused by cell interactions in the neighbourhood of the apex of bifurcation.

Moreover numerical simulations of non-Newtonian models were performed around the bifurcation at the regions 1–5 (see Fig. 7).

Figures 8 and 9 show the velocity profiles for both computational and experimental results before and after the bifurcation, respectively.

Figures 8 and 9 suggest that the RBCs velocities close to the microchannel wall are higher than that obtained with the numerical models since slip at the walls of the channel was assumed to be non-existent in the latter case. It is well known, in microcirculation and other areas [4, 5, 13, 20, 28, 32], that RBCs, macromolecules, colloids, etc., are excluded from the region of the channel with low velocity and this may explain the observed differences.

Moreover, Figs. 8 and 9 confirm [35] that the velocity profiles obtained with the power law model ( $n = 0.6$ ) are more flat than the ones obtained with the Newtonian model ( $n = 1$ ). For infinite pseudoplasticity ( $n = 0$ ) a plug flow should be obtained [35]. It is important to note that in Figs. 8 and 9 the average velocity obtained with the different constitutive equations was the same.

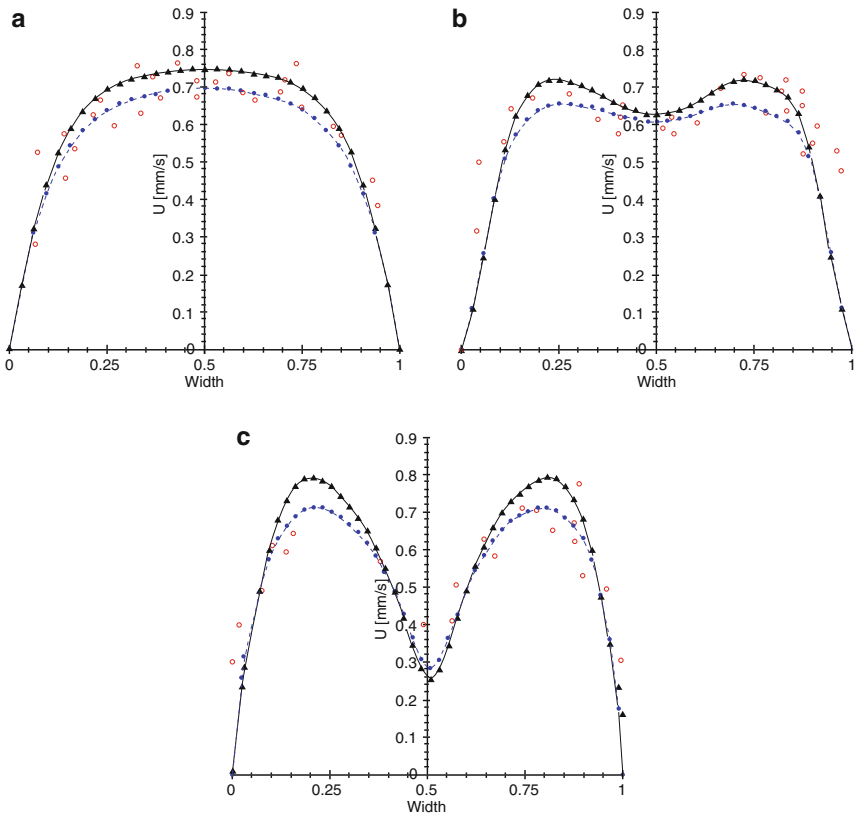


**Fig. 8** Velocity profiles for both computational and experimental results before the bifurcation: (a) region 1; (b) region 2; (c) region 3. (—) Newtonian; (---●) Power Law; (—▲) Carreau Model; (○) Confocal micro-PTV RBC velocities

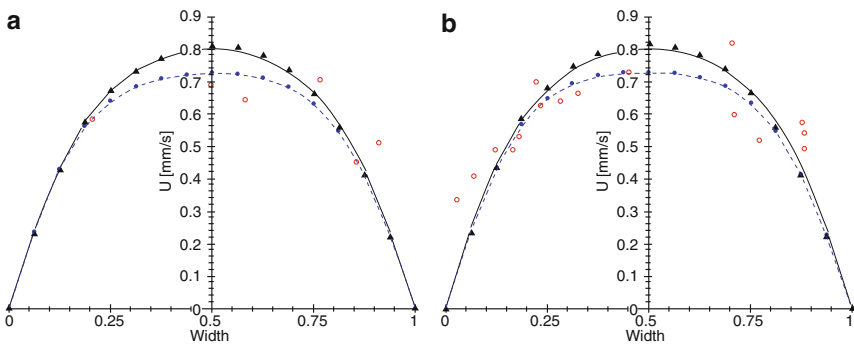


**Fig. 9** Velocity profiles for both computational and experimental results after the bifurcation: (a) region 4; (b) region 5. (—) Newtonian; (---●) Power Law; (—▲) Carreau Model; (○) Confocal micro-PTV RBC velocities

## 4 Limitations and Future Directions

The primary goal of the present work is to provide new insights on the rheological properties of blood in microvascular network models. To accomplish it experimental flow studies was performed with a confocal micro-PTV system complemented with the most recent advances in microfabricated technologies. However, the soft-lithography quality is strongly dependent not only on the photolithography methodology but also on the photomask resolution and its fidelity to the original design. In the present work we used a plastic photomask and according to our preliminary results we found small discrepancies between the tested *in vitro* model and the original design. Although these discrepancies were not taken into account in the present study we are aware about the possible influence of them on the results shown. Hence, in the future we are planning to carry on the current research by taking into account such discrepancies.

*In vitro* experimentation has the potential to provide a more realistic information on the flow properties of blood when compared with numerical simulations. However, once validated the numerical models can be a valuable tool to obtain more detailed insights about the blood rheological properties in microvascular networks. Generally, there are two major approaches to model of the non-Newtonian nature of blood [33]. One is based on the conventional continuum approach, in which a blood constitutive equation is assumed such as the casson model and the power-law model [36]. A more complex and realistic approach is based on a multiphase approach, in which the blood is considered as a multiphase suspension of deformable particles and where levels of submodeling for the behaviour of blood components are introduced. Some examples for this type of approach are the boundary element method [23, 26, 34], the immersed boundary method [2, 7, 24, 31], the lattice Boltzmann method [6, 29] and the moving particle semi-implicit (MPS) method [19, 30]). Recent reviews on these numerical methods can be found in Liu et al. [18], Yamaguchi et al. [33] and Lima et al. [14]. Although the multiphase flow approach is a very promising method it requires massive computational power. Hence, only recently this latter approach is being actively pursued due to the advances of the computational techniques and the computing power.

In the current study we have only performed simulations by using a continuum computational approach to model of the non-Newtonian nature of blood. However for the size of the microchannel used in presented work we can not neglect the effect of the suspension of deformable cells on its flow behaviour. Hence, we expect in a near future to compare the obtained experimental results with multi-phase numerical models.

## 5 Conclusions

A confocal micro-PTV system for the analysis of the complex phenomena happening at bifurcations was proposed. The system was complemented by a soft-lithography technique to fabricate the *in vitro* models and by a continuum computational model approach to study the non-Newtonian nature of the working fluids.

Qualitative experimental observations suggested that RBC paths around the bifurcation apex seems to suffer small deviations from the streamlines of the plasma flow probably due to cell interactions enhanced by the high local Hct originated at this region.

The simulations performed with a finite-element computational fluid dynamics (CFD) program POLYFLOW emphasized the need of developing a multiphase approach.

**Acknowledgements** This study was supported in part by the following grants: Grant-in-Aid for Science and Technology (BII/UNI/0532/EME/2008, PTDC/SAU-BEB/108728/2008, PTDC/SAU-BEB/105650/2008 and PTDC/EME-MFE/099109/2008) from the Science and Technology Foundation (FCT) and COMPETE, Portugal and Grant-in-Aid for Scientific Research (S) from the Japan Society for the Promotion of Science (JSPS; No.19100008). We also acknowledge the support from the 2007 Global COE Program “Global Nano-Biomedical Engineering Education and Research Network”. The authors would like also to thank Dr. C. Balsa for his valuable assistance and support for the MATLAB numerical calculations and Ms. B. Oliveira, Ms. D. Cidre and Mr. M. Lagoela for their valuable technical assistance in this research work.

## References

1. Abramoff, M., Magelhaes, P., Ram, S.: Image processing with image J. *Biophotonics Int.* **11**, 36–42 (2004)
2. Bagchi, P.: Mesoscale simulation of blood flow in small vessels. *Biophys. J.* **92**, 1858–1877 (2007)
3. Chien, S., Usami, S., Skalak, R.: Blood flow in small tubes In: Renkins, M., Michel, C.C. (eds.) *Handbook of Physiology—The Cardiovascular System IV*, pp. 217–249. American Physiological Society, Bethesda (1984)
4. Dias, R.P.: Size fractionation by slalom chromatography and hydrodynamic chromatography. *Recent Patents Eng.* **2**, 95–103 (2008)
5. Dias, R.P., Fernandes, C.S., et al.: Starch analysis using hydrodynamic chromatography with a mixed-bed particle column, *Carbohydr. Polym.* **74**, 852–857 (2008)
6. Dupin, M.M., Halliday, I., et al.: Modeling the flow of dense suspensions of deformable particles in three dimensions. *Phys. Rev. E.* **75**, 066707 (2007)
7. Eggleton, C.D., Popel, A.S.: Large deformation of red blood cell ghosts in a simple shear flow. *Phys. Fluids.* **10**, 1834–1845 (1998)
8. Fernandes, C.S., Dias, R.P., et al.: Simulation of stirred yoghurt processing in plate heat exchangers. *J. Food Eng.* **69**, 281–290 (2005)
9. Fernandes, C.S., Dias, R.P., et al.: Laminar flow in chevron-type plate heat exchangers: CFD analysis of tortuosity, shape factor and friction factor. *Chem. Eng. Process.: Process Intensif.* **46**, 825–833 (2007)
10. Fernandes, C.S., Dias, R.P., et al.: Friction factors of power-law fluids in plate heat exchangers. *J. Food Eng.* **89**, 441–447 (2008)
11. Goldsmith, H., Turitto, V.: Rheological aspects of thrombosis and haemostasis: Basic principles and applications. *ICTH-Report-Subcommittee on Rheology of the International Committee on Thrombosis and Haemostasis. Thromb. Haemost.* **55**, 415–435 (1986)
12. Johnston, B.M., Johnston, P.R., et al.: Non-Newtonian blood flow in human right coronary arteries: Steady state simulations. *J. Biomech.* **37**, 709–720 (2004)
13. Lima, R., Ishikawa, T., et al.: Measurement of individual red blood cell motions under high hematocrit conditions using a confocal micro-PTV system. *Ann. Biomed. Eng.* **37**, 1546–1559 (2009)

14. Lima, R., Ishikawa, T., et al.: Blood flow behavior in microchannels: Advances and future trends. In: *Single and Two-Phase Flows on Chemical and Biomedical Engineering*. Bentham (in press) (2011)
15. Lima, R., Wada, S., et al.: Confocal micro-PIV measurements of three dimensional profiles of cell suspension flow in a square microchannel. *Meas. Sci. Tech.* **17**, 797–808 (2006)
16. Lima, R., Wada, S., et al.: In vitro confocal micro-PIV measurements of blood flow in a square microchannel: The effect of the haematocrit on instantaneous velocity profiles. *J. Biomech.* **40**, 2752–2757 (2007)
17. Lima, R., Wada, S., et al.: In vitro blood flow in a rectangular PDMS microchannel: Experimental observations using a confocal micro-PIV system. *Biomed. Microdevices* **2**(10), 153–167 (2008)
18. Liu, W.K., Liu, Y., et al.: Immersed finite element method and its applications to biological systems. *Comput. Methods Appl. Eng.* **195**, 1722–1749 (2006)
19. Kondo, H., Imai, Y., et al.: Hemodynamic analysis of microcirculation in malaria infection. *Ann. Biomed. Eng.* **37**, 702–709 (2009)
20. Maeda, N.: Erythrocyte rheology in microcirculation. *Jpn. J. Physiol.* **46**, 1–14 (1996)
21. Meijering, E., Smal, I., Danuser, G.: Tracking in molecular bioimaging. *IEEE Signal Process. Mag.* **3**(23), 46–53 (2006)
22. Oliveira, B., Lagoela, M., et al.: Analyses of the blood flow in a microchannel with a bifurcation. In: *Proceedings of 3<sup>o</sup> Congresso Nacional de Biomecânica, Bragança, Portugal* (2009)
23. Omori, T., Ishikawa, T. et al.: Behavior of a red blood cell in a simple shear flow simulated by a boundary element method, In: *Proceedings of Bioengineering 08, London, UK* (2008)
24. Peskin, C.S.: Numerical analysis of blood flow in the heart. *J. Comput. Phys.* **25**, 220–233 (1977)
25. Popel, A., Johnson, P.: Microcirculation and hemorheology. *Annu. Rev. Fluid Mech.* **37**, 43–69 (2005)
26. Pozrikidis, C.: Numerical simulation of the flow-induced deformation of red blood cells. *Ann. Biomed. Eng.* **31**, 1194–1205 (2003)
27. Pries, A., Secomb, T., et al.: Resistance to blood flow in microvessels in vivo. *Circ. Res.* **75**, 904–915 (1994)
28. Small, H.: Hydrodynamic chromatography a technique for size analysis of colloidal particles. *J. Colloid. Interface Sci.* **48**, 147–161 (1974)
29. Succi, S.: *The Lattice Boltzmann Equation for Fluid Mechanics and Beyond*, Clarendon Press, Oxford (2001)
30. Tsubota, K., et al.: Particle method for computer simulation of red blood cell motion in blood flow. *Comp. Methods Programs Biomed.* **83**, 139–146 (2006)
31. Univerdi, S.O., Tryggvason, G.: A front-tracking method for viscous, incompressible multi-fluid flows. *J. Comput. Phys.* **100**, 25–37 (1992)
32. Venema, E., Kraak, J.C., et al.: Packed-column hydrodynamic chromatography using 1- $\mu$ m non-porous silica particles. *J. Chromatogr. A* **740**, 159–167 (1996)
33. Yamaguchi, T., Ishikawa, T., et al.: Computational blood flow analysis – new trends and methods. *J. Biomech. Sci. Eng.* **1**, 29–50 (2006)
34. Youngren, G.K., Acrivos, A.: Stokes flow past a particle of arbitrary shape: A numerical method of solution. *J. Fluid Mech.* **69**, 377–403 (1975)
35. Wilkinson, W.L.: *Non-Newtonian fluids: Fluid mechanics, mixing and heat transfer*, pp. 61–63. Pergamon Press, London (1960)
36. Zhang, J.B., Kuang, Z.B.: Study on blood constitutive parameters in different blood constitutive equations. *J. Biomech.* **33**, 355–360 (2000)